

## Eastern Kentucky University Encompass

---

EKU Faculty and Staff Scholarship

---


3-2003

# Enrichments of $^{34}\text{S}$ in sulfide minerals of deep-water marine sediments of the Blake Ridge, offshore southeastern United States

Kathryn G. Takacs  
*Eastern Kentucky University*

Walter S. Borowski  
*Eastern Kentucky University*

Follow this and additional works at: [https://encompass.eku.edu/fs\\_research](https://encompass.eku.edu/fs_research)

 Part of the [Biogeochemistry Commons](#), [Geochemistry Commons](#), [Geology Commons](#), [Sedimentology Commons](#), and the [Stratigraphy Commons](#)

---

### Recommended Citation

Takacs, K.G., W.S. Borowski, 2003. Enrichments of  $^{34}\text{S}$  in sulfide minerals of deep-water marine sediments of the Blake Ridge, offshore southeastern United States. EKU Graduate Research Papers.

This Conference Presentation is brought to you for free and open access by Encompass. It has been accepted for inclusion in EKU Faculty and Staff Scholarship by an authorized administrator of Encompass. For more information, please contact [Linda.Sizemore@eku.edu](mailto:Linda.Sizemore@eku.edu).

**Enrichments of  $^{34}\text{S}$  in sulfide minerals of deep-water marine  
sediments of the Blake Ridge,  
offshore southeastern United States**

**Kathryn Gauthier Takacs**

**(Candidate, Master of Science)**

**and**

**Walter S. Borowski**

**(Assistant Professor, Department of Earth Sciences)**

**Submitted to ECU Sigma Xi Chapter**

**14 March 2003**

## ABSTRACT

Past research shows that active sulfide mineralization occurs at the base of the sulfate reduction zone (SRZ) in modern, deep-water, continental-margin sediments that overlie methane gas hydrate. These sulfide minerals (elemental sulfur, S<sup>0</sup>; iron monosulfides, ~FeS; and pyrite, FeS<sub>2</sub>) are enriched in <sup>34</sup>S because of sulfate reduction and anaerobic methane oxidation (AMO) processes occurring above and near the sulfate-methane interface (SMI).

The data in this study show that 5 discrete zones of sulfide minerals are preserved in a 703.8-meter sediment column associated with methane gas hydrate. These zones of sulfide minerals are also enriched in <sup>34</sup>S. The shallowest zone is the present-day SMI, and we infer that the other 4 zones are past locations of the SMI.

Today, enrichments of <sup>34</sup>S in sulfide minerals occur because of anaerobic methane oxidation (AMO) carried out by methanotrophs and sulfate-reducing microbes in areas that have significant methane delivery to the SMI in methane gas hydrate terranes. Thus, these <sup>34</sup>S enrichments are a diagenetic indicator that point out occurrences of high methane delivery to the sulfate-methane interface and the action of the AMO consortium. From the data, we infer that these conditions exist not only today, but also have existed at several discrete times since the mid-Miocene, when sulfur isotopic composition of sulfide minerals is similar to or heavier than that occurring today.

## INTRODUCTION

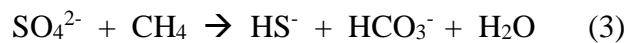
A decimeters- to meters-thick layer in the sediment column known as the sulfate-methane interface (SMI) exists at varying depths below the seafloor within continental-margin, deep-water sediments. Different biogeochemical processes occur above, below and at the SMI. Above this interface, sulfate is found at high concentration in pore waters; below this interface sulfate is absent or at low concentration because sulfate is depleted by the biogeochemical process of sulfate reduction:



in which microbes use sulfate to oxidize organic matter (e.g., Berner, 1980). Below the interface, methane occurs within pore waters because it is produced by methanogenic microbes:



(e.g., Berner, 1980). A unique biogeochemical process called anaerobic methane oxidation (AMO):

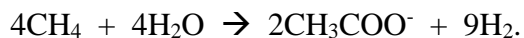


(Reeburgh, 1976) occurs at the interface.

There are two pathways for sulfate depletion. If little methane is present below the SMI, the decomposition of organic matter (Eq. 1) is the dominant sulfate depletion process. If methane flux is significant, sulfate consumption by AMO (Eq. 3) becomes the dominant process. The amount of sulfate depletion through AMO depends on the amount of methane delivered to the SMI from the sediments below.

A symbiotic association of at least two microbial groups, methanotrophs (methane consumers) and sulfate reducers (sulfate consumers) (e.g., Orphan, et al., 2001), create an intertwined sulfur and carbon cycle at the SMI through AMO (Figure 1).

Methanotrophs, members of *Archaea*, consume methane to produce organic molecules, usually acetate ( $\text{CH}_3\text{COO}^-$ ). A possible half-reaction for this process is:



Sulfate-reducing bacteria then consume the resultant acetate:



to produce dissolved carbon dioxide and hydrogen sulfide. It is the production of hydrogen sulfide, ultimately derived from sulfate through sulfate depletion, that is the source for sulfide mineralization within the sulfate reduction zone and at the sulfate-methane interface.

## Previous Research

Site 995 was drilled into sediments of the Blake Ridge, off the coast of South Carolina, as part of Ocean Drilling Program (ODP) Leg 164 (Figure 2). Sulfate profiles of pore waters from this site show steep linear gradients, which strongly suggest that larger amounts of sulfate are being consumed by AMO at the base of the sulfate reduction zone (Figure 3) (Borowski et al., 1996, 1999). Alkalinity and total dissolved carbon dioxide ( $\Sigma\text{CO}_2$ ) increase with depth, then alkalinity shows an increase at the SMI due to the local addition of  $\text{CO}_2$  by AMO. The carbon isotopic composition of  $\Sigma\text{CO}_2$  is lightest (enriched in  $^{12}\text{C}$ , depleted in  $^{13}\text{C}$ ) at the SMI, indicating that a large component of the carbon within the  $\text{CO}_2$  pool is derived from methane.  $\delta^{13}\text{C}$  values of the  $\Sigma\text{CO}_2$  pool are as depleted as -38‰ Pee Dee Belemnite (PDB). These values combined with diagenetic modeling suggest that at least 35% of the pore water sulfate is consumed by AMO (Borowski et al., 2000a; Hoehler et al., 2000). Such elevated levels of AMO can only occur with large methane flux from below the SMI.

The data in this paper represent a first test to a hypothesis that contends that similar zones of  $^{34}\text{S}$  enrichment will occur within authigenic sulfide minerals that formed at past locations of the sulfate-methane interface. We measure the concentration of authigenic sulfide minerals as well as determine the magnitude of their sulfur isotopic composition, within a 700-meter thick sedimentary column that currently contains extensive deposits of methane gas hydrates. We then document the stratigraphic patterns of the concentration and isotopic data.

## METHODS AND PROCEDURE

We use squeezed sediment samples to extract sulfide sulfur from sediments at ODP Site 995 (Leg 164, Blake Ridge area), an area that is underlain by extensive methane gas hydrate deposits (Paull, Matusumoto, Wallace, et al., 1996) (Figure 2). There are 197 squeeze-cake samples collected throughout Holes A and B from ODP Site 995, which reached a total depth of 704.6 meters with a maximum age of late Miocene (6.14 Ma) (Paull, et al., 1996). Sediment samples are ground into a uniform powder in order to measure the amount of sulfide sulfur residing with bulk sulfide minerals and its sulfur isotopic composition ( $\delta^{34}\text{S}$ , relative to the Canyon Diablo Troilite, CDT). To date we have measured the sulfide sulfur content of 60 samples and have measured the sulfur isotopic composition of 64 samples.

Sulfide sulfur is extracted from solid-phase sulfide minerals ( $\text{S}^{\circ}$ ,  $\text{FeS}$ ,  $\text{FeS}_2$ ) using the chromium reduction method of Canfield, et al. (1986). The first step in this procedure involves amalgamating solid mossy zinc in a solution of 75 ml mercuric chloride and 925 ml of 6N hydrochloric acid (HCl). The amalgamated zinc is placed in a large empty plastic wash bottle with a 1M solution of chromic chloride ( $\text{CrCl}_3$ ) and 2M HCl, and nitrogen gas ( $\text{N}_2$ ) is flushed

through Tygon plastic tubing into the wash bottle to evacuate atmospheric gases. After about 15 minutes, the green  $\text{CrCl}_3$  has turned to cobalt blue. This indicates reduction from  $\text{Cr}^{+3}$  to  $\text{Cr}^{+2}$ . A small piece of tubing is attached to the output of the wash bottle, and a 60 ml syringe is used to withdraw solution. Under a fume hood, an apparatus consisting of 4 distillation tubes is connected in series by Tygon tubing to allow cold water to cool the distillation tubes.  $\text{N}_2$  gas is flushed through narrow tubing into the distillation tubes and into flasks containing approximately 1 gram of sediment sample, 10 ml ethanol, and 30 ml of reduced  $\text{CrCl}_3$  solution, and 10 ml 6N HCl. This mixture is then boiled to  $\sim 200^\circ \text{C}$  with a hot plate placed under each sample sediment flask. As hydrogen sulfide gas ( $\text{H}_2\text{S}$ ) is released from the sediment, it is flushed by  $\text{N}_2$  through narrow tubing into 4 individual trapping flasks, which contain 30 ml of a 0.136 M zinc acetate ( $\text{ZnAc}$ ) and 0.36 M ammonium hydroxide ( $\text{NH}_4\text{OH}$ ) solution or 30 ml of a 0.1M silver nitrate ( $\text{AgNO}_3^-$ ) solution. After approximately 2 hours, the reaction has completely extracted all of the sulfide in the sample, and the  $\text{N}_2$  is turned off.

In order to measure the amount of sulfide sulfur, zinc sulfide ( $\text{ZnS}$ ) precipitate is digested with 10 ml of 6N HCl, and titrated in the trapping flask with a potassium iodate/potassium iodide solution (10.700 g  $\text{KIO}_3$ , 50.0 g KI, dissolved in 500 ml of distilled  $\text{H}_2\text{O}$ ) to measure the concentration of sulfide sulfur in the sediment contained within authigenic sulfide minerals. For sulfur isotopic measurements, another aliquot of sediment is run through the apparatus a second time, using the same procedure, only in this run the trapping medium is silver nitrate ( $\text{AgNO}_3$ ). The resulting precipitate (silver sulfide,  $\text{Ag}_2\text{S}$ ) can be directly used for sulfur isotopic analysis. The  $\text{Ag}_2\text{S}$  is filtered, dried and weighed in order to calculate the concentration of sulfur present. The precipitate is then stored in a labeled scintillation vial. Approximately 0.1 g of the  $\text{Ag}_2\text{S}$  was sent to the Environmental Isotope Laboratory (University of Waterloo, Ontario) for sulfur

isotopic analysis using a gas chromatograph-mass spectrometer and following the general method of Holt and Engelkemeir (1970).

## **RESULTS**

We looked for zones of sulfide mineralization in sediments from two holes from Site 995, ODP Leg 164. Samples from this site were relatively random, and spanned the entire length of each hole. For each sample, we measured the concentration of sulfide sulfur from authigenic sulfide minerals, as well as their isotopic composition. The sulfide sulfur concentration data show five discrete zones of enrichment in authigenic sulfide minerals (arrows, Figure 4), and the isotopic composition data show five zones of relative enrichment in  $^{34}\text{S}$  (arrows, Figure 4). These five zones are correlative and are based on sulfur isotopic compositions that are near or exceed 0 ‰ CDT. There are other peaks of sulfide sulfur concentration higher than background levels that are correlative to samples with sulfur isotopic composition more negative than 0 ‰ CDT. The shallowest peak of sulfide sulfur concentration and  $\delta^{34}\text{S}$  enrichment occurs at the present-day sulfate methane interface (SMI) as shown in Figure 4.

## **DISCUSSION**

Sulfide minerals are preserved in the sedimentary record, and their sulfur isotopic signature should also be preserved, providing clues to the biogeochemical processes responsible for sulfide mineralization. The isotopic composition of sulfide minerals at the present day SMI shows enrichment in  $^{34}\text{S}$  relative to background levels produced by sulfur disproportionation and sulfate reduction occurring in the sediment above the SMI (Figure 4; Borowski et al., 2000b, Figure 5).



## Sulfate Depletion and Sulfide Production

Sulfate concentration decreases with depth (Figure 4) as sulfate is depleted by two principal diagenetic reactions. Sulfate-reducing bacteria consume sulfate and use it to oxidize sedimentary organic matter. Sulfate is also consumed at the SMI through AMO. Both processes produce interstitial, dissolved sulfide ( $\Sigma\text{HS}^- = \text{H}_2\text{S}, \text{HS}^-, \text{S}^{2-}$ ) in a zone known as the sulfate reduction zone (SRZ) above the SMI. Sulfate  $\delta^{34}\text{S}$  values become more positive deeper within the sediments as sulfate reducers preferentially remove sulfate with  $^{32}\text{S}$ . This causes the sulfate pool to become enriched in  $^{34}\text{S}$  near the SMI. Interstitial sulfate located just above the SMI at Site 995 has a maximum enrichment in  $\delta^{34}\text{S}$  of +51.6‰ CDT. The magnitude of this enrichment is 30.6‰ CDT (Borowski et al., 2000b) compared to the  $\delta^{34}\text{S}$  of modern seawater (+21‰ CDT; Rees et al., 1978).

Borowski et al. (2000b) identified three main zones of sulfide transformations in the sediments of the Blake Ridge. In the uppermost SRZ, sulfide produced from sulfate reduction of organic matter is transformed into elemental sulfur ( $\text{S}^0$ ) and is then disproportionated into sulfate and dissolved sulfide by microbes:



(Canfield and Thamdrup, 1994). This sulfate is enriched in  $^{32}\text{S}$  (depleted in  $^{34}\text{S}$ ) relative to the initial sulfate, because it is derived from dissolved sulfide, which is enriched in  $^{32}\text{S}$  due to preferential uptake of  $^{32}\text{S}$  versus  $^{34}\text{S}$  by microbes during sulfate reduction (Goldhaber and Kaplan, 1980). As sulfur disproportionation continues to recycle sulfate from the sulfide pool back into sulfate reduction, the sulfide will become increasingly depleted in  $^{34}\text{S}$ . The isotopic signal of severe  $^{34}\text{S}$  depletion is transmitted into sulfide minerals (elemental sulfur,  $\text{S}^0$ ; iron

monosulfides, FeS; pyrite, FeS<sub>2</sub>) because the fractionation from dissolved sulfide to solid-phase sulfide is only about 1‰ (Price and Shieh, 1979). These depletions can be as extreme as -50‰ CDT, and will form the background, or baseline signal for δ<sup>34</sup>S of sulfide minerals.

As sulfate becomes enriched in <sup>34</sup>S deeper within the sulfate reduction zone (Figure 3), the sulfide pool becomes concomitantly enriched in <sup>34</sup>S as well. However, the sulfide pool remains greatly enriched in <sup>32</sup>S relative to the sulfate pool due to the large isotopic fractionation involved in sulfate reduction (α=1.029-1.059; Chambers and Trudinger, 1978). Thus the sulfide minerals forming from interstitial sulfide in the sulfate reduction zone will be enriched in <sup>34</sup>S relative to background levels created by sulfur disproportionation.

Sulfate is maximally enriched in <sup>34</sup>S at the SMI. Maximally <sup>34</sup>S-enriched sulfate consumed by AMO creates sulfide maximally enriched in <sup>34</sup>S, and this <sup>34</sup>S-enriched sulfide signal is transmitted to the sulfide minerals created at the SMI. Because AMO is such an important process in methane-rich sediments, larger amounts of sulfide and sulfide minerals can be produced at the SMI above a large source of methane. This causes more sulfide minerals enriched in <sup>34</sup>S to be added to the background sulfur isotopic signal created in the sediments above the SMI.

### **Non-Steady State Deposition**

During steady-state deposition of marine sediments, the SMI remains stationary at the same depth below the sediment-water interface. As deposition occurs, sediment formed at the sediment-water interface will be buried, passing successively through the sulfate reduction zone, and through the SMI deeper into the sediment column. Thus, any <sup>34</sup>S enrichments created by

AMO, sulfide production, and sulfur mineralization at the SMI will be "smeared" throughout the sediment column disguising any authigenic sulfide formation occurring at the SMI.

A stratigraphically stationary, long-lived SMI will add larger amounts of sulfide minerals enriched in  $^{34}\text{S}$  (e.g., Raiswell, 1988). This scenario should produce a sharp peak in  $\delta^{34}\text{S}$ , so that sulfide mineralization produced at the SMI can be recognized within the stratigraphic record.

The magnitude of sulfide sulfur concentration and  $\delta^{34}\text{S}$  enrichment above background levels will thus depend on how long the SMI remains stationary through geologic time. As discussed above, the amount of methane delivery to the SMI will also control the rate of AMO and the rate of sulfide mineral formation.

### **The Stratigraphic Record**

The isotopic composition of sulfide minerals below the present-day SMI show  $^{34}\text{S}$  enrichment at discrete zones, and these zones correlate with zones of enrichment in sulfide mineral concentration (Figure 4). These zones, observed below the present-day SMI, have sulfur properties that are consistent with formation at SMIs during the geologic past that have been successfully preserved in the stratigraphic record.

### **Implications**

If these  $^{34}\text{S}$  enrichments within sulfide minerals have indeed formed at paleo-SMIs, then they record specific processes occurring in specific settings in the geologic past. Significant levels of methane delivery to the SMI are responsible for increasing rates of AMO and increasing the proportion of interstitial sulfate depleted by co-consumption with methane. This means that sediments associated with  $^{34}\text{S}$  enrichments were methane rich, implying a high

activity level of sulfate reducers and *Archaea* comprising the AMO consortium. Moreover, if temperature and pressure conditions were suitable for gas hydrate formation, the enrichments may also identify the presence of gas hydrates in the past (Borowski et al., 1999).

## CONCLUSION

Present-day sulfate-methane interfaces with significant  $^{34}\text{S}$  enrichments within bulk sulfide minerals (elemental sulfur,  $\text{S}^0$ ; iron monosulfides,  $\sim\text{FeS}$ ; and pyrite,  $\text{FeS}_2$ ) indicate significant methane delivery to the SMI and identify a diagenetic environment where sulfate reducers and *Archaea* (methanotrophs?) mediate the diagenetic process of anaerobic methane oxidation. Enrichments of  $^{34}\text{S}$  within the sulfide mineral phases deeper in the sedimentary section should likewise indicate significant methane flux in the geologic past.  $^{34}\text{S}$  enrichments larger than those observed at the present-day SMI may identify periods of higher methane flux and/or non-steady state deposition when the SMI remains stratigraphically-stationary over an interval of geologic time. Both conditions cause larger amounts of sulfide minerals enriched in  $^{34}\text{S}$  continue to accumulate at the SMI. Thus, "paleo-SMIs", like those formed today, identify a diagenetic environment with significant amounts of interstitial methane and perhaps the occurrence of gas hydrates, provided that conditions of temperature and pressure are conducive to their formation.

## REFERENCES

- Berner, R.A. 1980, Early Diagenesis: A Theoretical Approach. Princeton: Princeton University Press, 241 pp.
- Borowski, W.S., Paull, C.K., Ussler W. III, 2002, The meeting of two microbial worlds: Geochemistry of the sulfate-methane interface. In: K. White and E. Urquhart (Eds.), ODP's Greatest Hits, Volume 2, 1pp. [Online]. Available from the World Wide Web: <http://www.joiscience.org/greatesthits2/pdfs/borowski.pdf>.
- Borowski, W.S., Hoehler, T.M., Alperin, M.J., Rodriguez, N.M., and Paull, C.K., 2000a, Significance of anaerobic methane oxidation in methane-rich sediments overlying the Blake Ridge gas hydrates. In: C.K. Paull, R. Matsumoto, P.J. Wallace, and W.P. Dillon, *Proceedings ODP, Scientific Results*, 164: Ocean Drilling Program, College Station, Texas, p. 87-99.
- Borowski, W.S., C.K. Paull, and William Ussler III, 2000b, Geologic implications of sulfide mineralization at the sulfate-methane interface in marine sediments: *GSA Abstracts Programs*, v. 32(7), A-256.
- Borowski, W.S., Paull, C.K., Ussler W. III, 1999, Global and local variations of interstitial sulfate gradients in deep-water, continental margin sediments: Sensitivity to underlying methane and gas hydrates: *Marine Geology*, v. 159, p. 131-154.
- Borowski, W.S., Paull, C.K., Ussler W. III, 1996, Marine pore-water sulfate profiles indicate *in situ* methane flux from underlying gas hydrate: *Geology*, v. 24, p. 655-658.
- Canfield, D.E., Raiswell, R., Westrich, J.T., Reaves, C.M., and Berner, R.A., 1986, The use of chromium reduction in the analysis of reduced inorganic sulfur in sediments and shales: *Chemical Geology*, v. 54, p. 149-155.
- Canfield, D.E., and Thamdrup, B., 1994, The production of  $^{34}\text{S}$ -depleted sulfide during bacterial disproportionation of elemental sulfur: *Science*, v. 266, p. 1973-1975.
- Chambers, L.A., and Trudinger, P.A., 1978, Microbiological fractionation of stable sulfur isotopes: A review and critique: *Geomicrobiology Journal*, v. 1, p. 249-293.
- Goldhaber, M.B., and Kaplan, I.R., 1980. Mechanisms of sulfur incorporation and isotope fractionation during early diagenesis in sediments of the Gulf of California. *Marine Chemistry*, 9: 95-143.
- Hoehler, T.M., Borowski, W.S., Alperin, M.J., Rodriguez, N.M., and Paull, C.K., 2000, Model, stable isotope and radiotracer characterization of anaerobic methane oxidation in gas-hydrate-bearing sediments of the Blake Ridge, in Paull, C.K., Matsumoto, R., Wallace, P.J., and Dillon, W.P., *Proceedings ODP, Scientific Results*, 164: College Station, TX, Ocean Drilling Program, p. 79-85.

- Holt, B.D., and Engelkemeir, A.G., 1970, Thermal decomposition of barium sulfate to sulfur dioxide for mass spectrometric analysis: *Analytical Chemistry*: v. 42, p. 1451-1453.
- Orphan, V.J., House, C.H., Hinrichs, K.U., McKeegan, K.D., and DeLong, E.F., 2001, Methane-consuming Archaea revealed by directly coupled isotopic and phylogenetic analysis: *Science*, v. 293, p. 484-487.
- Paull, C.K., Matsumoto, R., Wallace, P. et al., 1996, *Proceedings ODP, Initial Reports*, 164, Ocean Drilling Program, College Station, Texas.
- Price, F.T., and Shieh, Y.N., 1979, Fractionation of sulfur isotopes during laboratory synthesis of pyrite at low temperatures: *Chemical Geology*, v. 27, p.245-253.
- Raiswell, R., 1988, Chemical model for the origin of minor limestone-shale cycles by anaerobic methane oxidation: *Geology*, v. 16, p. 641-644.
- Reeburgh, W.S., 1976, Methane consumption in Cariaco Trench waters and sediments: *Earth and Planetary Science Letters*, v. 28, p. 337-344.
- Rees, C.E., Jenkins, W.J., and Monster, J., 1978, The sulfur isotopic composition of ocean water sulfate: *Geochimica et Cosmochimica Acta*, v. 42, p. 377-381.

## FIGURES WITH FIGURE CAPTIONS

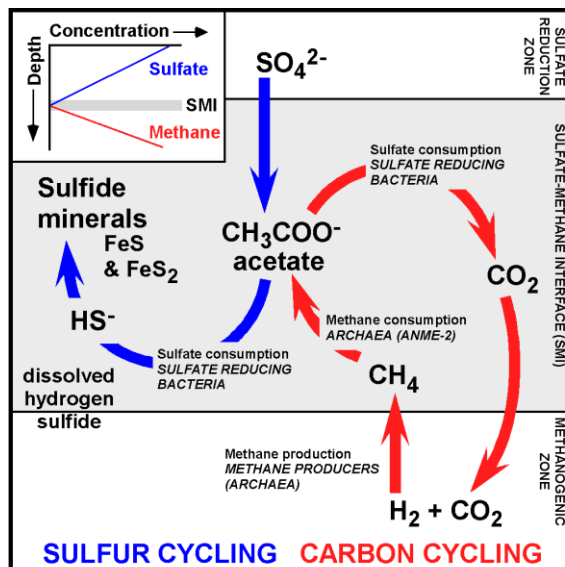


**Figure 1.** Sulfate and methane diffuse through marine sediments to the sulfate-methane interface (SMI). Here, methane is consumed by methanotrophs (*Archaea*) to produce organic molecules (e.g., acetate), which are then consumed by sulfate reducers (*Bacteria*), producing dissolved sulfide that is quickly precipitated as sulfide minerals within the sediments. The amount of sulfate consumption depends on the amount of methane delivered to the SMI. Figure after Borowski et al. (2002).

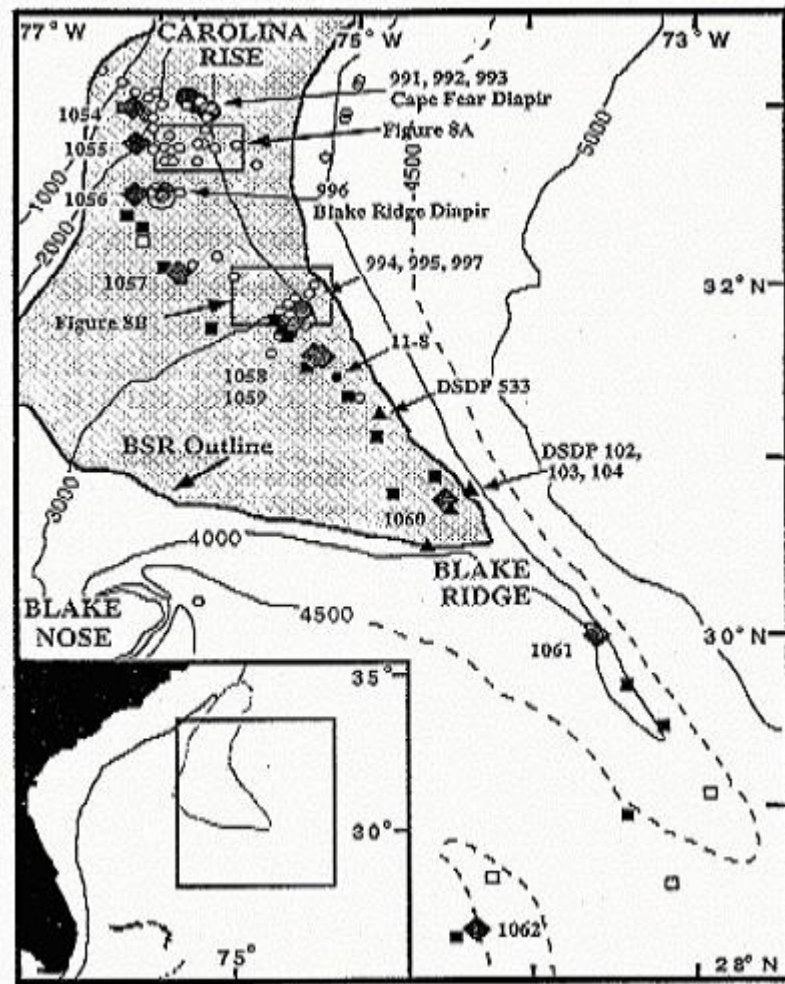


**Figure 2.** Map showing piston core, DSDP, and ODP sites of the Carolina Rise and Blake Ridge. From: Borowski, et al. (1999).



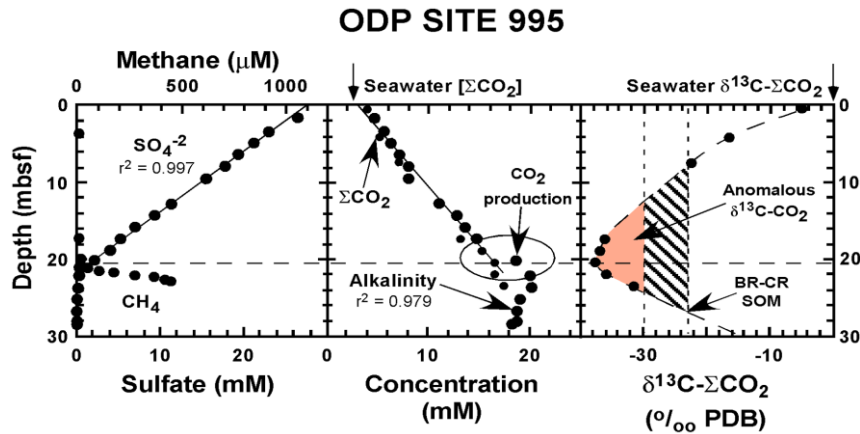


**Figure 3.** Concentration and isotopic profiles of sulfate, dissolved carbon dioxide, ( $\Sigma\text{CO}_2$ ), methane ( $\text{CH}_4$ ), alkalinity, and  $\delta^{13}\text{C}-\Sigma\text{CO}_2$  in ODP core 995 (Borowski et al., 2000b). Measurement uncertainties are less than symbol size. The circled portion in the middle section highlights local production of dissolved  $\text{CO}_2$  shown by a local increase in alkalinity. The shaded portion of the  $\delta^{13}\text{C}-\Sigma\text{CO}_2$  profile illustrates methane carbon in the  $\text{CO}_2$  pool that was definitely derived from methane through anaerobic methane oxidation. The hatched portion of the curve shows carbon likely derived from methane. The lower boundary of the curve is defined by a data point (-9.9‰) at 37.65 meters below seafloor (mbsf) that is not shown.

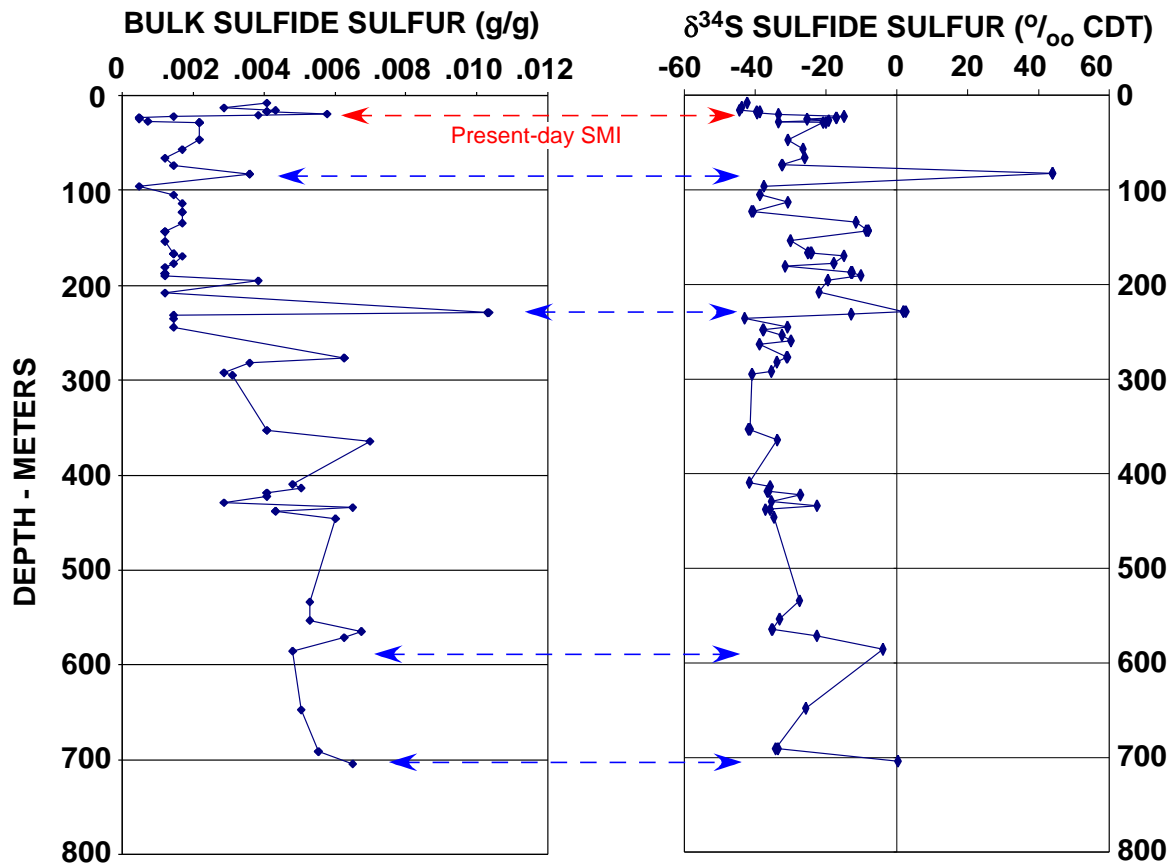


**Figure 7.** Graph showing the amount of sulfide sulfur (grams sulfide sulfur per weight sediment) residing in bulk sulfide minerals (elemental sulfur,  $\text{S}^0$ ; iron monosulfides,  $\sim\text{FeS}$ , and pyrite,  $\text{FeS}_2$ ) versus depth (left); and graph showing the sulfur isotopic composition ( $\delta^{34}\text{S}$ ) of bulk sulfide minerals relative to the CDT standard (Canyon Diablo Troilite) versus depth (right).

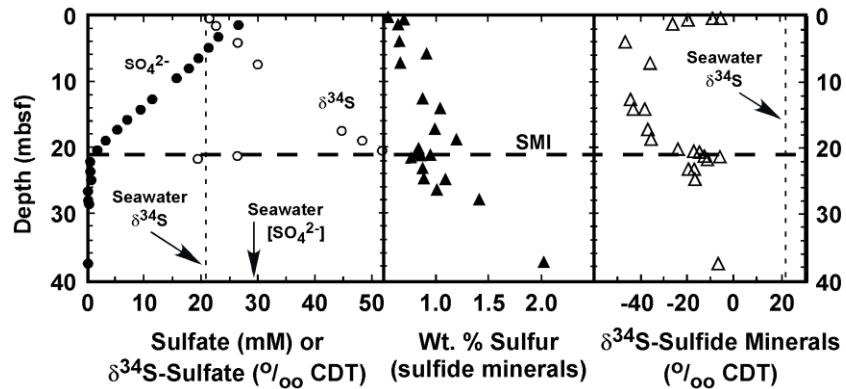


**Figure 5.** Profiles of interstitial dissolved sulfate, sulfur isotopic composition of interstitial sulfate in per mil (‰) relative to the Canyon Diablo Troilite (CDT), sulfur content of sediments residing in sulfide minerals ( $S^0$ ,  $FeS$ ,  $FeS_2$ ) expressed in weight percent elemental sulfur, and sulfur isotopic composition of authigenic sulfide minerals at ODP Site 995 (Borowski et al., 2000b). The concentration of sulfate in seawater and its sulfur isotopic composition are shown by dashed vertical lines. Dashed horizontal lines indicate the sulfate-methane interface (SMI), as defined by interstitial sulfate and methane concentrations. Sulfate concentrations from the ODP sites are from Paull, Matsumoto, Wallace, et al., (1996).